

Global Disk Oscillations in Binary Be Stars

Finny OKTARIANI

Department of Cosmoscience, Graduate School of Science, Hokkaido University, Kita-ku, Sapporo 060-0810, Japan
finny@astro1.sci.hokudai.ac.jp

and

Atsuo T. OKAZAKI

Faculty of Engineering, Hokkai-Gakuen University, Toyohira-ku, Sapporo 062-8605, Japan

(Received 2008 0; accepted 2008 0)

Abstract

We study the effects of the tidal interaction with the companion, via orbital separation and binary mass ratio, on the global one-armed oscillation modes in disks around binary Be stars. Our model takes into account the three-dimensional effect that contributes to the mode confinement, which was recently found by Ogilvie (2008). We find that the one-armed oscillations are well confined in systems with disks larger than a few tens of stellar radii. In such systems, the oscillation period depends little on the binary parameters. On the other hand, in systems with smaller disks, where the mode confinement is incomplete, the oscillation period increases with increasing orbital separation and/or decreasing binary mass ratio. The eigenmode is insensitive to the spectral type of the central star. Our results suggest that the dependence of V/R oscillation period on the orbital separation and binary mass ratio should be observed only in short period binary systems, and that, for systems with a similar orbital period, those with higher mass ratios will show shorter V/R variations.

Key words: stars: binaries: general, stars: emission-line, Be, stars: oscillations

1. Introduction

Be stars are non-supergiant B-type stars whose spectra show, or have at some time shown, one or more Balmer lines in emission (Collins 1987). A Be star is a rapidly rotating, B-type star as the central star with a two-component circumstellar envelope, a polar wind and an equatorial disk. The polar wind is a low-density, fast outflow emitting UV radiation. The wind structure is well explained by the line-driven wind model (Castor et al. 1975; Friend & Abbott 1986). On the other hand, the equatorial disk is a geometrically thin, high-density plasma in nearly Keplerian rotation (e.g., Porter & Rivinius 2003), from which the optical emission lines and the IR excess arise. Although there are still several competing scenarios for the Be disk formation, the most promising one is the scenario where the disk is formed by viscous accretion of gas ejected from the central star (Lee et al. 1991; see also Porter & Rivinius 2003, and references therein).

Many Be stars show long-term variations in their spectra over years to decades. One of these phenomena is called long-term V/R variations, which are variations of the ratio of relative intensity of violet (V) and red (R) peaks of a double-peaked emission line profile. The period of the long-term V/R variations is typically in the range 5-10 yr for isolated Be stars. It is widely accepted that the long-term V/R variations are attributed to global one-armed (i.e., the azimuthal wave number $m = 1$) oscillations in the Be disk (e.g., Porter & Rivinius 2003). It is based on the fact that in a nearly Keplerian disk a one-armed mode shows up as a very slowly revolving per-

turbation pattern (e.g., Kato 1983). The early versions of the one-armed oscillation model (Okazaki 1991, 1997; Papaloizou et al. 1992; Savonije & Heemskerk 1993) qualitatively well explained the observed characteristics of the V/R variations. However, owing to the lack of the mechanism for confining the modes to the inner part of the disk and the high sensitivity of the oscillation period on various parameters, the model had little predictive power (Firt & Harmanec 2006).

Recently, the model was advanced greatly. Ogilvie (2008) has solved the mode confinement problem by investigating a three-dimensional effect on the mode characteristics. While previous versions of the model had assumed motions to be independent of height since the disk is geometrically thin, he argued that the variation of the vertical gravitational acceleration around an elliptical orbit excites an oscillatory vertical motion in an eccentric disk that should not be neglected. Ogilvie (2008) showed that the three-dimensional effect alone allows confined prograde modes.

Hitherto, theoretical studies of one-armed oscillation modes in Be disks are mostly limited to isolated Be stars. However, according to the current census, the fraction of Be stars found in binary systems is $\sim 1/3$ (Porter & Rivinius 2003). The presence of the companion is most likely to change some features of the global one-armed oscillations in Be disks. Actually, in Be/X-ray binaries, which consist of a neutron star and an early-type Be star, the time-scale of V/R variations is frequently about 1 yr, which is much shorter than the typical V/R time-scale for isolated Be stars (e.g., Reig et al. 2005).

Moreover, there are observationally two types of long-term V/R variations in binary Be stars (Štefl et al. 2007). One is quasi-periodic V/R variations, where V/R peak ratio varies quasi periodically, which shows no correlation with their orbital phase. This type of V/R variations are similar to those usually observed for V/R variations in isolated Be stars. The other type is periodic V/R variations locked to the orbital period. This characteristic is found only in binary Be star systems. Unfortunately, no theoretical explanation is available yet for the phase-locked V/R variations.

In this paper, we investigate the effects of the companion on the characteristics of one-armed oscillation modes in binary Be stars, taking into account the tidal effects in addition to the three-dimensional effect. For simplicity, we assume the binary orbit to be circular. We find that the mode is well confined in disks larger than a few tens of stellar radii, which is consistent with Ogilvie (2008). In smaller disks, however, the mode confinement is incomplete and the oscillation period depends on the binary parameters significantly.

The structure of this paper is as follows. In section 2, we describe the unperturbed disk and derive the basic equations for linear, one-armed perturbations, following the formulation by Ogilvie (2008). The boundary conditions to be adopted are also discussed. In section 3, we present our numerical results, and in section 4, we compare our results with the observational features of V/R variations in binary Be stars. The final section is devoted to conclusions.

2. Basic equations for $m = 1$ density waves

2.1. Basic equations

As an unperturbed state, we take a geometrically thin, axisymmetric disk that locally rotates at a nearly Keplerian speed and is in hydrostatic equilibrium in the vertical direction. Because of the strong photoionization heating from the stellar radiation, this Be disk is taken to be isothermal at $0.6T_{\text{eff}}$ (Carciofi & Bjorkman 2006), where T_{eff} is the effective temperature of the central star. For simplicity, we assume the binary orbit to be circular and neglect the advective motion and viscous effects in the Be disk.

We use the cylindrical coordinate system (r, ϕ, z) . The equation of continuity and the equation of motion are respectively given by

$$\frac{\partial \rho}{\partial t} + \nabla \cdot (\rho \mathbf{v}) = 0 \quad (1)$$

and

$$\left[\frac{\partial}{\partial t} + (\mathbf{v} \cdot \nabla) \right] \mathbf{v} = -\nabla \Psi - \nabla h. \quad (2)$$

Here \mathbf{v} is the velocity vector, Ψ is the gravitational potential, and $h = c_s^2 \ln \rho$ is the enthalpy of an isothermal gas, where c_s is the isothermal sound speed and ρ is the density.

As far as eigenmode oscillations are concerned, we may

consider only the azimuthally averaged tidal potential (Hirose & Osaki 1993). We also take into account the rotational deformation of the rapidly rotating Be star, including only monopole and quadrupole term (Papaloizou et al. 1992). The potential in the disk midplane, Ψ_m , is then reduced to

$$\Psi_m \simeq -\frac{GM_1}{r} \left[1 + k_2 \left(\frac{\Omega_1}{\Omega_c} \right)^2 \left(\frac{r}{R_1} \right)^{-2} \right] - \frac{GM_2}{D} \left[1 + \frac{1}{4} \left(\frac{r}{D} \right)^2 \right], \quad (3)$$

where M_1 , R_1 and Ω_1 are the mass, radius and angular rotation speed of the Be star, k_2 and $\Omega_c = \sqrt{GM_1/R_1^3}$ are its apsidal motion constant and critical angular rotation speed, M_2 is the mass of the companion, and D is the binary separation. In equation (3), the first term is the gravitational potential of the Be star, in which the quadrupole contribution due to the rotational distortion of the star is taken into account, and the second term is the azimuthally averaged tidal potential.

In circular binaries with small mass ratios ($M_2/M_1 \lesssim 0.3$), a viscous disk is truncated at the tidal radius given by

$$R_{\text{tides}} \sim 0.9R_L \quad (4)$$

(Whitehurst & King 1991). Here R_L is the Roche lobe radius of the Be star given approximately by

$$R_L = D \frac{0.49q^{-2/3}}{0.69q^{-2/3} + \ln(1 + q^{-1/3})} \quad (5)$$

(Eggleton 1983), where $q = M_2/M_1$ is the binary mass ratio. In this paper, we thus assume that the Be disk is truncated at $r = R_{\text{tides}}$.

The unperturbed equilibrium state of the isothermal disk is given by

$$\rho = \rho_m(r) \exp\left(-\frac{z^2}{2H^2}\right), \quad (6)$$

$$\mathbf{v} = [0, r\Omega(r), 0], \quad (7)$$

$$p = c_s^2 \rho, \quad (8)$$

and

$$r\Omega^2 = \frac{d\Psi_m}{dr} + c_s^2 \frac{d \ln \rho_m}{dr}, \quad (9)$$

where $\Omega(r)$ is the angular frequency of disk rotation, $\rho_m(r)$ is the midplane density, and $H(r) = c_s/\Omega_K$ with $\Omega_K = \sqrt{GM_1/r^3}$ is the scale-height of the disk.

From equations (3) and (9), we have the explicit form of Ω as follows.

$$\Omega = \left(\frac{GM_1}{r^3} \right)^{1/2} \left\{ 1 - \frac{q}{2} \left(\frac{r}{D} \right)^3 + k_2 f^2 \left(\frac{R_1}{r} \right)^2 + \left(\frac{d \ln \rho_m}{d \ln r} \right) \left(\frac{H}{r} \right)^2 \right\}^{1/2}, \quad (10)$$

where $f = \Omega_1/\Omega_c$. Then, the associated local epicyclic frequency $\kappa(r)$ is explicitly written as

$$\begin{aligned} \kappa &= \left[2\Omega \left(2\Omega + r \frac{d\Omega}{dr} \right) \right]^{1/2} \\ &= \left(\frac{GM_1}{r^3} \right)^{1/2} \left\{ 1 - 2q \left(\frac{r}{D} \right)^3 - k_2 f^2 \left(\frac{R_1}{r} \right)^2 \right. \\ &\quad \left. + \left[2 \left(\frac{d \ln \rho_m}{d \ln r} \right) + \frac{d^2 \ln \rho_m}{d \ln r^2} \right] \left(\frac{H}{r} \right)^2 \right\}^{1/2}. \end{aligned} \quad (11)$$

On the above unperturbed state, we superpose a linear, $m = 1$ isothermal perturbation in the form of normal mode of frequency ω , which varies as $\exp[i(\phi - \omega t)]$. The linearized perturbed equations are then obtained as follows.

$$i(\Omega - \omega)v'_r - 2\Omega v'_\phi = -\frac{\partial h'}{\partial r}, \quad (12)$$

$$i(\Omega - \omega)v'_\phi + \frac{\kappa^2}{2\Omega}v'_r = -\frac{i h'}{r}, \quad (13)$$

$$i(\Omega - \omega)v'_z = -\frac{\partial h'}{\partial z}, \quad (14)$$

$$\begin{aligned} i(\Omega - \omega)h' + v'_r \frac{\partial h}{\partial r} + v'_z \frac{\partial h}{\partial z} \\ = -c_s^2 \left[\frac{1}{r} \frac{\partial(rv'_r)}{\partial r} + \frac{iv'_\phi}{r} + \frac{\partial v'_z}{\partial z} \right], \end{aligned} \quad (15)$$

where (v'_r, v'_ϕ, v'_z) and h' are the perturbed velocity and enthalpy, respectively.

In order to take the three-dimensional effect into account, we expand perturbed quantities in the z -direction in terms of Hermite polynomials as

$$v'_r(r, z) = \sum_n u_n(r) H_n(\zeta), \quad (16)$$

$$v'_\phi(r, z) = \sum_n v_n(r) H_n(\zeta), \quad (17)$$

$$v'_z(r, z) = \sum_n w_n(r) H_{n-1}(\zeta), \quad (18)$$

$$h'(r, z) = \sum_n h_n(r) H_n(\zeta) \quad (19)$$

(Ogilvie 2008; see also Okazaki et al. 1987), where $H_n(\zeta)$ is the Hermite polynomial defined by

$$H_n(\zeta) = \exp\left(\frac{\zeta^2}{2}\right) \left(-\frac{d}{d\zeta}\right)^n \exp\left(-\frac{\zeta^2}{2}\right) \quad (20)$$

with $\zeta = z/H$ being a dimensionless vertical coordinate and $n = 0, 1, 2, \dots$

The system of resulting equations is not closed because the equation for u_n refers to the higher order term h_{n+2} , which depends on u_{n+2} , the equation for which in turn refers to h_{n+4} , and so forth. Following Ogilvie (2008), we close the system of resulting equations by assuming $u_n \equiv 0$ for $n \geq 2$. Neglecting u_2 compared to u_0 is equivalent to assuming that the eccentricity of perturbed orbit of each gas particle is independent of z . If h_2 is also neglected, then we will obtain the two-dimensional equations. The

basic equations for linear $m = 1$ perturbations in inviscid disks are then given as follows.

$$2i(\omega_{\text{pr}} - \omega)u_0 = -\frac{dh_0}{dr} - \frac{2h_0}{r} + \frac{3h_2}{r}, \quad (21)$$

$$i\Omega \frac{h_0}{c_s^2} - \frac{u_0}{2r} + \frac{1}{r\Sigma} \frac{d(r\Sigma u_0)}{dr} = 0, \quad (22)$$

$$-i\Omega \frac{h_2}{c_s^2} + \frac{3u_0}{2r} = 0, \quad (23)$$

where $\Sigma = (2\pi)^{1/2} \rho_m H$ is the surface density and ω_{pr} is the local apsidal precession frequency given by

$$\begin{aligned} \omega_{\text{pr}} &= \Omega - \kappa \\ &\simeq \left(\frac{GM_1}{r^3} \right)^{1/2} \left\{ \frac{3}{4} q \left(\frac{r}{D} \right)^3 + k_2 f^2 \left(\frac{R_1}{r} \right)^2 \right. \\ &\quad \left. - \frac{1}{2} \left[\left(\frac{d \ln \rho_m}{d \ln r} \right) + \frac{d^2 \ln \rho_m}{d \ln r^2} \right] \left(\frac{H}{r} \right)^2 \right\}. \end{aligned} \quad (24)$$

In deriving equations (21)-(23), we have used approximations $|\omega| \ll \Omega$, $|\Omega - \kappa| \ll \Omega$, and $(c_s/r\Omega)^2 \ll 1$. Note that these equations are essentially the same as equations (A6)-(A8) of Ogilvie (2008), except that our equations implicitly depend on the tidal effect through Ω and κ .

Eliminating h_2 from equations (21) and (23), we have

$$\frac{dh_0}{dr} = -\frac{2}{r}h_0 + \left[2(\omega - \omega_{\text{pr}}) - \frac{9c_s^2}{2r^2\Omega} \right] iu_0, \quad (25)$$

and equation (22) is written as

$$i \frac{du_0}{dr} = \frac{\Omega}{c_s^2} h_0 - \left(\frac{1}{2} + \frac{d \ln \Sigma}{d \ln r} \right) \frac{i u_0}{r}. \quad (26)$$

We define Y_1 and Y_2 as $Y_1 = u_0$ and $Y_2 = -ih_0$. Then the basic equations to be solved are given by

$$\frac{dY_1}{dr} = \frac{\beta}{r} Y_1 + \frac{\Omega}{c_s^2} Y_2 \quad (27)$$

and

$$\frac{dY_2}{dr} = 2 \left[\omega - \left(\omega_{\text{pr}} + \frac{9c_s^2}{4r^2\Omega} \right) \right] Y_1 - \frac{2}{r} Y_2, \quad (28)$$

where $\beta = -1/2 - (d \ln \Sigma / d \ln r)$. Note that as shown by Ogilvie (2008), the term $9c_s^2 / 4r^2\Omega$ results from the three-dimensional effect and provides an important contribution to the confinement of the $m = 1$ modes.

2.2. Boundary conditions

We now consider the boundary conditions for equations (27) and (28). In Be stars with growing or persistent equatorial disks, material is likely injected continuously from the star to the disk, so there is no gap between the star and the disk. Since the pressure scale-height of the Be star near the interface is much smaller than that of the disk, the oscillations cannot penetrate the stellar surface. Hence, throughout this paper, we take the rigid wall boundary condition at the disk inner radius, i.e., $v'_r = 0$ at $r = R_1$, except in section 3.4 where we study the effect

of the free inner boundary condition. With $Y_1 = u_0$, this condition is written as

$$Y_1 = 0 \quad \text{at} \quad r = R_1. \quad (29)$$

In our model the Be disk is truncated at the tidal radius. Hence, we take the free boundary condition at the outer boundary. This condition is written as

$$\Delta p = 0, \quad (30)$$

where Δp is the Lagrangian perturbation of pressure. Given that the Eulerian perturbation of pressure, p' , varies as $\exp[i(\phi - \omega t)]$, equation (30) can be written as

$$i(\Omega - \omega)p' + v'_r \frac{\partial p}{\partial r} + v'_z \frac{\partial p}{\partial z} = 0. \quad (31)$$

Using the same procedure as in the previous subsection, we have

$$i(\Omega - \omega)h_0 + u_0 \frac{c_s^2}{\rho} \frac{\partial \rho}{\partial r} + u_0 c_s^2 \frac{\partial \ln H}{\partial r} = 0, \quad (32)$$

where we have used $h' = p/\rho$. Finally, with $Y_1 = u_0$ and $Y_2 = -ih_0$, we have the outer boundary condition as

$$(\Omega - \omega)Y_2 - \frac{d \ln \Sigma}{d \ln r} \frac{c_s^2}{r} Y_1 = 0 \quad \text{at} \quad r = R_{\text{tides}}. \quad (33)$$

3. Numerical results

We solve basic equations (27) and (28) for a range of parameters, including binary separation D ($10R_1 \leq D \leq 50R_1$) and binary mass ratio q ($q = 0.1$ and 0.3), with the boundary conditions described above. In the following calculations, we take a B0V star with $M_1 = 17.5M_\odot$, $R_1 = 7.4R_\odot$, and $T_{\text{eff}} = 30000\text{K}$ (Cox 2000) as the Be star model, except in section 3.3 where we consider a B5V star to study the spectral dependence of the mode characteristics. As for the quadrupole parameter, we take $k_2 f^2 = 5 \times 10^{-3}$ as a representative value, although there is a large uncertainty of this parameter in the range $k_2 f^2 = 2 \times 10^{-3} - 10^{-2}$, as discussed in the next section.

The pressure gradient force in our isothermal disk model depends solely on the radial density distribution. In the following we take the power-law disk density distribution that varies as $\rho_m \propto r^{-7/2}$, which is the theoretical density distribution of steady, isothermal decretion disks (Porter 1999; Okazaki 2001; Carciofi & Bjorkman 2006).

In this section, we study the effect of orbital separation in section 3.1 and that of binary mass ratio in section 3.2. We then briefly discuss the results for B5V stars in section 3.3 and the effect of the free inner boundary condition in section 3.4.

3.1. Effect of binary separation

In order to study the effect of binary separation on the oscillation characteristics of the Be disk in circular binaries, we vary the value of the binary separation D from $D = 10R_1$ to $D = 50R_1$, with binary mass ratio $q = 0.1$.

Figures 1 and 2 show the fundamental mode (left) and the first overtone (right) for $D = 10R_1$ and $D = 50R_1$, respectively. The top panels in each figure show the eigenfunction Y_1 ($= u_0$) (solid line) and Y_2/c_s^2 ($= -ih_0/c_s^2 =$

$-i\rho_0/\rho$) (dashed line) in the radial direction. In the middle panels, the color-scale plot shows the surface density perturbation relative to the unperturbed surface density, Σ'/Σ , in the (r, ϕ) -plane: the red (blue) region has a positive (negative) density perturbation. The arrows superposed on the color-scale plot denote the velocity vectors associated with the mode. The disk itself rotates counter-clockwise. The bottom panels shows the density perturbation, ρ' , in the (r, z) -plane of the disk, at $\phi = 0$. Note that the modes are linear, so their normalization is arbitrary.

All modes in Figs. 1 and 2 have positive frequencies, that is, they are prograde modes, which precess in the direction of disk rotation. Figure 2 (left) shows that the fundamental mode is well confined in a large disk. However, as shown in Fig. 1 for $D = 10R_1$, when the binary separation is small, the confinement of the fundamental mode is weak, so the mode propagates over the whole disk. As for the first overtones, the confinement is weak: it is not confined well even for a wide binary with $D = 50R_1$. Note that these results are consistent with Ogilvie (2008) who showed that the 3-D theory allows prograde, fundamental modes to be confined within several tens of stellar radii in disks around isolated Be stars.

In the middle panels of Figs. 1 and 2, we note that perturbation pattern averaged in the vertical direction is similar to that for 2-D disk models around isolated Be stars, which have been extensively studied. We thus expect that the current model can also explain the observed line profile variability. In fact, the modal features suggest that when the violet (red) peak is stronger than the red (violet) peak, the line profile as a whole redshifts (blueshifts). This is a typical behavior of the observed line profile variability (e.g., Okazaki 1991).

The bottom panels of Figs. 1 and 2 show a new feature that has not been suggested by the previous 2-D studies: The density perturbation, $\rho'(r, z)$, does not always take the maximum in the disk midplane. The behavior of $\rho'(r, z)$ depends on that of the radial component of perturbed velocity, $u_0(r)$, as seen from equation (23). In regions where u_0 is negligible, ρ' is dominated by the contribution from h_0 , so $|\rho'|$ at a fixed radius has a maximum in the equatorial plane and decreases with vertical coordinate. In contrast, in regions where u_0 is not negligible, the contribution from h_2 becomes significant. Then, the density perturbation has a maximum at a vertical coordinate $z \sim (1-2)H$, not in the equatorial plane. In the first overtone, these patterns appear alternately in the radial direction.

The distribution of eigenfrequency is shown in Figure 3 as a function of binary separation normalized by the Be star radius, D/R_1 , for $q = 0.1$. Here and hereafter, we normalize the eigenfrequency ω by the stellar critical rotation frequency $\Omega_c = \sqrt{GM_1/R_1^3}$. The solid lines and the dashed lines denote the fundamental modes and the first overtones, respectively. The thick lines are for a B0V star (and the thin lines are for a B5V star discussed in section 3.3). Note that all modes are prograde modes. Note also that the oscillation period of the fundamental mode increases to an asymptotic value with increasing bi-

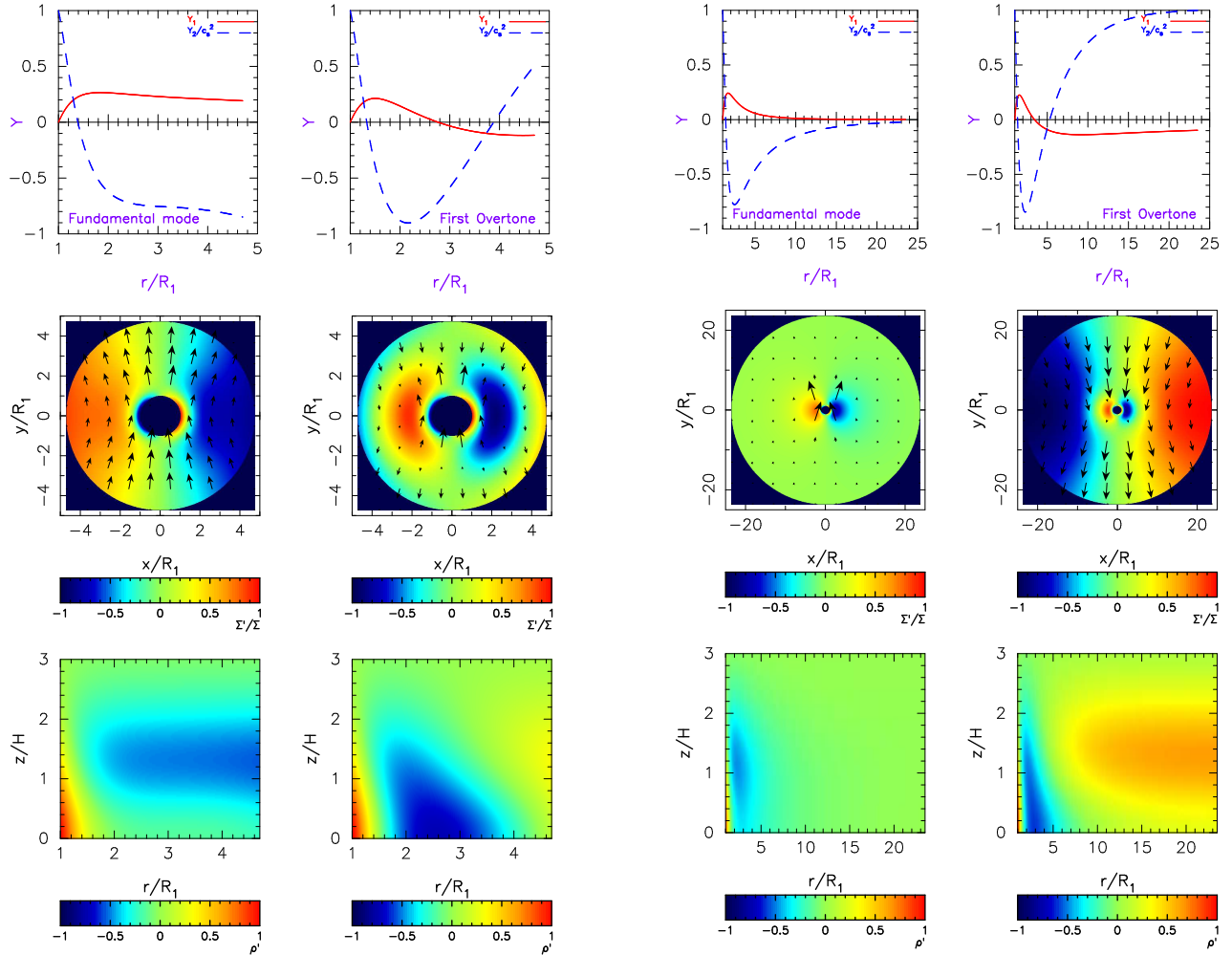


Fig. 1. Eigenfunctions of the $m=1$ fundamental mode (top left) and the first overtone (top right) for $D=10R_1$ and $q=0.1$ with the rigid inner boundary condition. The solid line denotes Y_1 , while the dashed line denotes Y_2/c_0^2 . In the middle panels, the color-scale plot show the surface density perturbation normalized by the unperturbed surface density, Σ'/Σ , in the (r, ϕ) -plane, while the arrows denote the perturbed velocity vectors. The bottom panels show the density perturbation, ρ' , in the (r, z) -plane at $\phi=0$.

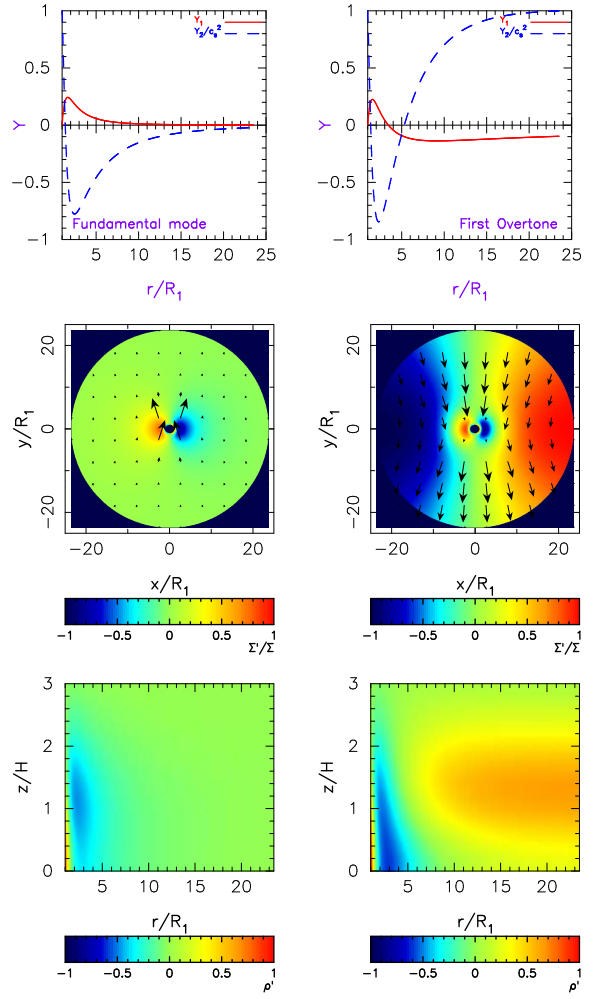


Fig. 2. Same as Fig. 1, but for $D=50R_1$.

nary separation: for a B0V star, it varies from 1.38 yr for $D=10R_1$ to 2.25 yr for $D=50R_1$. This is because the tidal field is weaker for larger orbital separations, and weaker tidal field decreases the local apsidal precession rate ω_{pr} [see eq. (24)]. The lower the local precession rate ω_{pr} , the lower the eigenfrequency ω . Thus, the eigenfrequency of the fundamental mode decreases with increasing orbital separation. However, the effect of the binary separation is only appreciable for small D/R_1 . In systems with large binary separation, the eigenfrequency of the fundamental mode changes little, because the mode is already well confined to the inner part of the disk, so the size of the disk does not matter anymore.

3.2. Effect of binary mass ratio

In order to study the effect of binary mass ratio on disk oscillation modes, we have performed calculations for $q=0.3$, in addition to the calculations for $q=0.1$ shown above. We have also carried out calculations for an artificial case with no tidal effect, except that the disk is truncated at the same radius as for $q=0.1$ (hereafter, called the $q=0$ case), to compare with the $q=0.1$ result.

Figure 4 shows the distribution of eigenfrequency as a

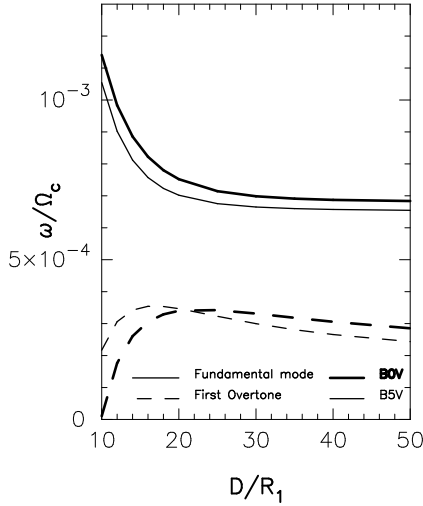


Fig. 3. Eigenfrequency as a function of normalized binary separation, D/R_1 , for $q = 0.1$. The solid lines denote the fundamental modes, while the dashed lines denote the first overtones. The thick lines and the thin lines are for a B0V star and a B5V star, respectively. ω is normalized by the stellar critical rotation frequency Ω_c . The rigid boundary condition is applied at the inner disk radius.

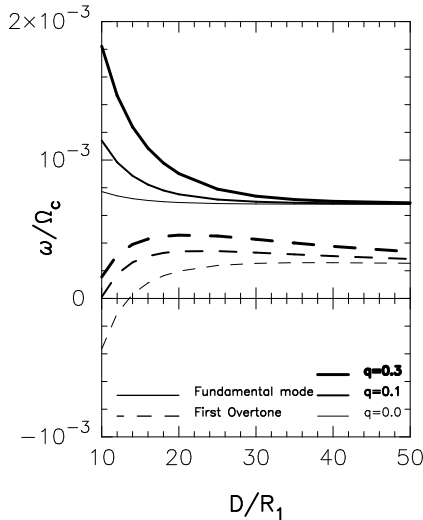


Fig. 4. Eigenfrequency as a function of normalized binary separation, D/R_1 , for $q = 0$ (thin lines), 0.1 (lines with intermediate thickness), and 0.3 (thick lines). The solid lines are for the fundamental modes, while the dashed lines are for the first overtones. ω is normalized by the stellar critical rotation frequency Ω_c . The rigid inner boundary condition is adopted.

function of normalized binary separation, D/R_1 , for $q = 0$ (thin lines), 0.1 (lines with intermediate thickness), and 0.3 (thick lines). The solid line and the dashed line denote the fundamental mode and the first overtone, respectively. It is noted that the eigenfrequency increases with increasing binary mass ratio. This is particularly the case for small D/R_1 . This is because the local apsidal precession rate ω_{pr} increases with increasing mass ratio q . As mentioned above, the higher ω_{pr} , the higher the eigenfrequency.

Here we compare our result with that of Ogilvie (2008). Ogilvie (2008) normalized the eigenfrequency ω and the quadrupole parameter $k_2 f^2$ by ϵ^2 , where $\epsilon = c_s(R_1/GM_1)^{1/2}$, which is $\sim 2.3 \times 10^{-2}$ in our case of the B0V star. Then, $k_2 f^2 = 5 \times 10^{-3}$ and $\omega/\Omega_c \sim 6.8 \times 10^{-4}$ for $q = 0$ and $D = 50R_1$ in our case corresponds to $\tilde{Q} \equiv k_2 f^2/\epsilon^2 \sim 9.1$ and $\tilde{\omega} \equiv \omega/\epsilon^2 \sim 1.3$, respectively. We note that this is consistent with $\tilde{\omega} \sim 1.2$ for $\tilde{Q} \sim 9$ as seen by eye from Fig. 3 (left) of Ogilvie (2008)).

Figure 4 suggests that the first overtones are retrograde modes, which precess in the opposite direction to disk rotation, for small binary separation ($D \sim 10R_1$) and very small mass ratio ($q \ll 0.1$). Note that the retrograde modes can exist in the Be disk in binaries because of its truncated outer radius.

3.3. Spectral type dependence

As shown by Firt & Harmanec (2006), the one-armed oscillation period depend also on the mass and radius of the central star. In this subsection, we discuss the effect of the spectral type. For this purpose, we calculated the eigenmodes for a B5V central star with $M_1 = 5.9M_\odot$, $R_1 = 3.9R_\odot$, and $T_{\text{eff}} = 15200\text{K}$ (Cox 2000).

Figure 3 compares the distribution of normalized eigenfrequency for two different spectral types, B0V (thick lines) and B5V (thin lines). From the figure, we note that the normalized eigenfrequency of the fundamental mode for a B5V star is slightly lower than that of a B0V star. This is because both the local apsidal precession rate ω_{pr} and the 3-D effect are smaller for a B5V star than for a B0V star: A B5V star has a higher critical rotation frequency Ω_c and a lower sound speed than a B0V star does. This decreases $\omega_{\text{pr}}/\Omega_c$. It also weakens the 3-D effect via a smaller value of $9c_s^2/4r^2\Omega$ in eq. (28). The same discussion is applied to the first overtone, except for small binary separation ($D \lesssim 20R_1$) where the tidal effect for a fixed value of q is relatively stronger for a B5V star than for a B0V star.

Because of a higher Ω_c of a B5V star, the dimensional eigenfrequency (or the oscillation period) shows the opposite trend. Although the normalized eigenfrequency is slightly lower for a B5V star than for a B0V star, the eigenfrequency itself shows the opposite trend. Oscillation period of the fundamental mode for a B5V star ranges from 0.96yr for $D = 10R_1$ to 1.5yr for $D = 50R_1$, which is slightly shorter than that for a B0V star by $\sim 30\%$.

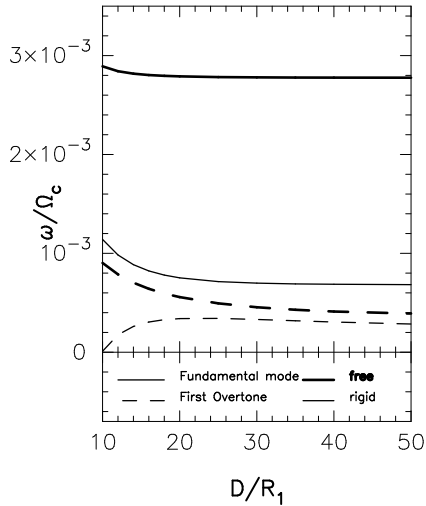


Fig. 5. Eigenfrequency as a function of normalized binary separation, D/R_1 , for free (thick lines) and rigid (thin lines) inner boundary condition. The solid lines are for the fundamental modes, while the dashed lines for the first overtones.

3.4. Free inner boundary condition

In long term, some Be stars change their state between the Be star phase and the normal B star phase. There are also other stars that show the loss and reformation of the high-velocity wings of emission lines (Rivinius et al. 2001). These observational features indicate that in these stars, the Be disk, or at least the inner part, is completely lost and then reformed (Porter & Rivinius 2003). In the formation stage, it is likely that the Be disk and the central star are directly connected. The rigid inner boundary condition is adequate for such a situation. In the dissipation stage, however, a gap is expected to open between the disk and the central star, owing to the accretion or ablation of the innermost part.

In order to study global oscillations in dissipating Be disks, we have performed calculations for the free inner boundary condition, which means that the Lagrangian perturbation of the pressure, Δp , vanishes at the disk inner radius. For simplicity, we have adopted the same unperturbed disk state as in the rigid boundary case. Using the same procedure as in section 2.2, the free inner boundary condition is written as

$$(\Omega - \omega)Y_2 - \frac{d \ln \Sigma}{d \ln r} \frac{c_s^2}{r} Y_1 = 0 \quad \text{at} \quad r = R_1. \quad (34)$$

Figure 5 shows the eigenfrequency distributions as a function of normalized binary separation, D/R_1 , for $q = 0.1$. The thick lines are for the free inner boundary condition, while the thin lines for the rigid inner boundary condition. The solid lines and the dashed lines denote the fundamental modes and the first overtones, respectively. We note that the eigenfrequency is higher and the mode is more concentrated in the inner part with the free inner boundary condition than with the rigid one, as first pointed out by Papaloizou & Savonije (2006) and then confirmed by Ogilvie (2008). As in the case of rigid inner

boundary condition, our result for $q = 0.0$ and $D = 50R_1$ with the free inner boundary condition is consistent with that of Ogilvie (2008).

4. Discussion

As mentioned in section 1, binary Be star systems show two types of long-term V/R variations. The first one is quasi-periodic V/R variations, similar to those observed in isolated Be stars. The second one is periodic V/R variations locked to their orbital period (Štefl et al. 2007). In our study, we have found only eigenmodes compatible with the former type of variations: our eigenmodes depend on the orbital period, but they are not locked to it. It is interesting to carry out numerical simulations to study whether tidally forced, nonlinear oscillations can explain the phase locked V/R variations, but this is beyond the scope of this paper.

In the previous section, we have shown how global one-armed oscillation modes depend on the binary parameters. The oscillation period becomes longer in the case of a wider binary separation and/or a lower binary mass ratio. Such dependence, however, will be observed only for short period binaries. In wide binaries where the disk size is large enough to confine the one-armed modes in the inner part of the disk, the mode characteristics depend little on the binary parameters. The critical orbital separation, where the size of the Be disk is just large enough to confine the fundamental mode, depends on the details of the model. The difference between the model oscillation periods (a few yr) and the observed ones (5-10 yr) implies that there are still missing mechanisms that affect the global disk oscillations. One of them could be the optically thick line forces examined by Gayley et al. (2001), who found that these forces have a net effect that likely lowers the eigenfrequency of the one-armed mode. The more realistic density and temperature distributions could also contribute to lower the eigenfrequency. However, despite these mechanisms not taken into account, we believe that the current results are qualitatively robust.

Observationally, no clear dependence of the V/R period on the binary parameters has been found. Reig et al. (2005) compared the time-scales of disk formation/dissipation cycle and V/R variability with the orbital period for eight Be/X-ray binaries (see their Table 3). They found a good correlation between the time-scale of disk formation/dissipation cycle and the orbital period, which agrees with the scenario that the Be disk is truncated by the tidal torques from the neutron star (Okazaki & Negueruela 2001). On the other hand, the V/R variability time-scale has no clear correlation with the orbital period, although short period systems have, in general, short V/R time-scale, with which our results qualitatively agree.

In this paper, we have assumed an inviscid disk for mathematical simplicity. However, viscosity in the Be disk is considered to play an important role in the formation of a nearly Keplerian disk by causing the outward drift of matter ejected from the equatorial surface of the Be star,

as proposed in the viscous decretion disk model by Lee et al. (1991). Negueruela et al. (2001) showed, after Kato et al. (1978), that global $m = 1$ modes, which are neutral in inviscid disks, become overstable when the viscous effect is taken into account as a perturbation. The growth rate of the mode, i.e., the imaginary part of the eigenfrequency, of the mode is proportional to the Shakura-Sunyaev viscosity parameter α , while the real part is independent of α as long as $\alpha \ll 1$. Ogilvie (2008) also obtained the result that the real part of an eigenfrequency in a viscous disk with $\alpha = 0.1$ is only slightly different from that in an inviscid disk. Thus, we expect that as far as the oscillation period is concerned, our result is valid for viscous disks with small α as well.

Finally, we briefly comment on the effect of stellar rotation via the quadrupole parameter $k_2 f^2$. For B-type main sequence stars, the stellar evolution calculations result in the apsidal motion constant k_2 in the range $2.5 \times 10^{-3} \leq k_2 \leq 10^{-2}$, depending on the evolutionary stage and the internal angular momentum distribution (Claret & Gimnez 1991; Claret 1995; Claret 1999). While it remains controversial how close the rotation of Be stars is to the critical rotation, it is likely $f = \Omega_1/\Omega_c \gtrsim 0.9$ (e.g., Frémat et al. 2005), which yields for the quadrupole factor in the range $2 \times 10^{-3} \lesssim k_2 f^2 \lesssim 10^{-2}$.

In order to study the effect, we have calculated the eigenmodes for $k_2 f^2 = 10^{-2}$, implicitly assuming an extremely high value of $k_2 \sim 10^{-2}$ for a critically rotating star ($f \sim 1$), for a B0V star in a binary with $q = 0.1$. As expected, the resulting eigenfrequency was higher than that for $k_2 f^2 = 5 \times 10^{-3}$: It increased from $\omega \sim 1.1 \times 10^{-3}$ to $\omega \sim 1.6 \times 10^{-3}$ for $D = 10R_1$ and from $\omega \sim 6.8 \times 10^{-4}$ to $\omega \sim 1.3 \times 10^{-3}$ for $D = 50R_1$. This is because the local apsidal precession rate ω_{pr} appreciably increases in the inner part with an increase in $k_2 f^2$. For the first overtones, we also found higher eigenfrequencies for the larger quadrupole parameter. However, the difference is much smaller than in the case of fundamental modes, in particular for systems with large orbital separations.

5. Conclusions

We have studied the tidal effect of the companion on the global oscillation modes in equatorial disks around binary Be stars. For simplicity, we assumed the binary orbit to be circular and the Be disk to be inviscid, isothermal, and truncated at the tidal radius. We solved linearized equations for global $m = 1$ perturbations in a three-dimensional Be disk with a power-law density distribution, with the rigid wall inner boundary condition, which is applicable to systems where material is ejected continuously, so there is no gap between the star and the disk.

We have obtained prograde fundamental modes even when the quadrupole contribution to the potential is negligible. This confirms the results of Ogilvie (2008). In our study of binary Be star systems, the modes are well confined when the disk is larger than a few tens of stellar radii.

We have found that the oscillation period increases

with increasing binary separation and/or decreasing binary mass ratio. The effect is, however, only appreciable for small binary separation. In systems with large binary separations, the fundamental mode is well confined to the inner part of the disk, so the eigenfrequency no longer depends on the binary parameters.

Be stars sometimes show a cavity between the star and the disk when the disk is being dissipated. In order to study the global oscillation modes in such disks, we have solved the perturbation equations with a free inner boundary condition, without changing the density distribution. We have obtained much higher eigenfrequencies with the free inner boundary condition than with the rigid one, as in Papaloizou & Savonije (2006) and Ogilvie (2008). The result implies an interesting possibility that the V/R variability time-scale is shorter when the disk is dissipating than when it is forming or persistent.

In this paper we have assumed a power-law density distribution. In the disk dissipation stage, however, it is likely that the density distribution is far from a power-law form and is highly peaked near the inner radius. In a subsequent paper, we will study the effect of density distribution on the global $m = 1$ oscillations.

FO thanks Masayuki Fujimoto for helpful discussions. She also acknowledges the scholarship from Ministry of Education, Culture, Sports, Science and Technology. We thank Gordon Ogilvie for kindly showing us his latest result on the three-dimensional effect on the $m = 1$ mode confinement.

References

- Carciofi, A.C., & Bjorkman, J.E., 2006, ApJ, 639, 1081
- Castor, J. I., Abbott, D. C., & Klein, R.I. 1975, ApJ, 195, 157
- Chen, H. & Marlborough, J.M. 1994, ApJ, 427, 1005
- Claret, A. 1995, A&AS, 109, 441
- Claret, A. 1999, A&A, 350, 56
- Claret, A. & Gimnez, A. 1991, A&AS, 87, 507
- Collins II, G.W. 1987, in IAU Colloq. 92, Physics of Be Stars, ed. A.Slettebak & T.P. Snow (Cambridge Univ. Press, Cambridge) p.3
- Cox, A.N. 2000, in Allen's Astrophysical Quantities Fourth Edition (The Athlone Press, London), p.389
- Eggleton, P. P. 1983, ApJ, 268, 368
- Frémat, Y., Zorec, J., Hubert, A.-M., & Floquet, M. 2005, A&A, 440, 305
- Firt, R. & Harmanec, P. 2006, A&A, 447, 277
- Friend, D. B. & Abbott, D. C. 1986, ApJ, 311, 701
- Gayley, K. G., Ignace, R., Owocki, S. P. 2001, ApJ, 558, 802
- Hirose, M., Osaki, Y. 1993, PASJ, 45, 595
- Kato, S. 1983, PASJ, 35, 249
- Kato, S. 1978, MNRAS, 185, 629
- Lee, U., Saio, H., Osaki, Y. 1991, MNRAS, 250, 432
- Negueruela I., Okazaki A.T., Fabregat J., Coe M.J., Munari U., Tomov T., 2001, A&A, 369, 117
- Ogilvie, G.I. 2008, MNRAS, in press
- Okazaki, A.T. 1991, PASJ, 43, 75
- Okazaki, A.T. 1997, A&A, 318, 548
- Okazaki, A.T. 2001, PASJ, 53, 119
- Okazaki, A. T., Kato, S, Fukue, J. 1987, PASJ, 39, 457

- Okazaki, A.T., Negueruela, I. 2001, *A&A*, 369, 108
- Papaloizou, J.C., Savonije, G.J., Henrichs, H.F. 1992, *A&A*, 265, L45
- Papaloizou, J.C.B., Savonije, G.J. 2006, *A&A*, 456, 1097
- Porter, J.M. 199, *A&A*, 348, 512
- Porter, J.M., Rivinius, T. 2003, *PASP*, 115, 1153
- Reig, P., Negueruela, I., Fabregat, J., Chato, R., Coe, M.J. 2005, *A&A*, 440, 1079
- Rivinius, Th., Baade, D., Štefl, S., Maintz, M. 2001, *A&A*, 379, 257
- Savonije, G.J., Heemskerk, M.H.M. 1993, *A&A*, 276, 409
- Štefl, S., Okazaki, A.T., Rivinius, T., Baade, D. 2007, in *ASP Conf. Series, Active OB Stars: Laboratories for Stellar & Circumstellar Physics* (Astronomical Society of the Pacific, San Francisco), p.274
- Telting, J.H., Heemskerk, M.H.M., Henrichs, H.F., Savonije, G.J. 1994, *A&A*, 288, 558
- Vakili, F., Mourard, D., Stee, PH., Bonneau, D., Berio, P., Chesneau, O., Thureau, N., Morand, F., Labeyrie, A., & Tallon-Bosc, I. 1998, *A&A*, 335, 261
- Whitefurst, R., King, A. 1991, *MNRAS*, 249, 25